NEOPLASIA
www.neoplasia.com

Volume 12 Number 7 July 2010 pp. 571–578 571

How Do Bisphosphonates Inhibit Bone Metastasis *In Vivo*?[1]

Pierrick G. Fournier*,†,2,3, Verena Stresing*,†,2, Frank H. Ebetino‡ and Philippe Clézardin*,†

*Institut National de la Santé et de la Recherche Médicale, UMR 664, IFR62, Lyon, France; †Université Lyon 1, Villeurbanne, France; ‡Warner Chilcott, Mason, OH, USA

Abstract

Bisphosphonates are potent inhibitors of osteoclast-mediated bone resorption and have demonstrated clinical utility in the treatment of patients with osteolytic bone metastases. They also exhibit direct antitumor activity *in vitro* and can reduce skeletal tumor burden and inhibit the formation of bone metastases *in vivo*. However, whether such effects are caused by a direct action of bisphosphonates on tumor cells or indirectly through inhibition of bone resorption remains unclear. To address this question, we used here a structural analog of the bisphosphonate risedronate, NE-58051, which has a bone mineral affinity similar to that of risedronate, but a 3000-fold lower bone antiresorptive activity. *In vitro*, risedronate and NE-58051 inhibited proliferation of breast cancer and melanoma cell lines. *In vivo*, risedronate and NE-58051 did not inhibit the growth of subcutaneous B02 breast tumor xenografts or the formation of B16F10 melanoma lung metastasis. In contrast to NE-58051, risedronate did inhibit B02 breast cancer bone metastasis formation by reducing both bone destruction and skeletal tumor burden, indicating that the antitumor effect of bisphosphonates is achieved mainly through inhibition of osteoclast-mediated bone resorption.

Neoplasia (2010) 12, 571–578

Introduction

Nitrogen-containing bisphosphonates (N-BPs), such as risedronate, are a class of antiresorptive drugs routinely used in the treatment of patients with lytic bone diseases, particularly metastatic disease [1–3]. Chemically, N-BPs share a common P-C-P structure, in which two phosphonate groups are linked to a central carbon atom [4]. This common backbone, together with one of the covalently bound side chains (preferably a hydroxyl group), are essential for binding to hydroxyapatite crystals in the skeleton [4]. Because of their high affinity for bone mineral, N-BPs quickly localize to the skeleton where they act primarily through the inhibition of osteoclast-mediated bone resorption, thus alleviating the tumor-associated bone destruction. The potency of an N-BP to inhibit osteoclast-mediated bone resorption is determined by the nitrogen-containing side chain, which interacts with farnesyl pyrophosphate synthase (FPPS), a key enzyme in the mevalonate pathway, thereby blocking the activity of this enzyme. This leads to the inhibition of the prenylation of small GTPases important for osteoclast cell functions and survival [5,6]. In addition, there is now extensive preclinical evidence that these agents exert direct antitumor effects *in vitro*, inhibiting tumor cell adhesion, invasion, and proliferation and inducing apoptosis [1,7]. They are also able to reduce skeletal tumor burden and inhibit the formation of bone metastases in a variety of animal models [8]. Furthermore, bisphosphonates may also act indirectly on tumor cells through antiangiogenic [9–11] and/or immunomodulatory mechanisms [12,13].

The exact mechanism(s) responsible for the observed antitumor effects of N-BPs in preclinical models remains unclear. Inhibition of osteoclast-mediated bone resorption by bisphosphonates leads to a reduced release of bone-derived growth factors, ultimately altering the bone microenvironment [14,15] and thus affecting the ability of tumor cells to grow in bone. It is therefore likely that the antitumor activity of N-BPs in bone is mainly caused by inhibition of osteoclast

Address all correspondence to: Verena Stresing, PhD, Faculté de Médecine Laennec, Institut National de la Santé et de la Recherche Médicale, U.664, Rue Guillaume Paradin, 69372 Lyon cedex 08, France. E-mail: vstresing@web.de

[1]This study was supported by Institut National de la Santé et de la Recherche Médicale, Université Claude Bernard Lyon-1, Alliance for Better Bone Health (Procter & Gamble Pharmaceuticals and Sanofi-Aventis), and Ligue Régionale contre le Cancer (P.C.). P.F. was a recipient of a fellowship from the Association pour la Recherche sur le Cancer.

[2]These authors contributed equally to this work.

[3]Current address: Division of Endocrinology and Metabolism, Department of Medicine, Indiana University, Indianapolis, IN.

Received 15 February 2010; Revised 15 February 2010; Accepted 23 April 2010

DOI 10.1593/neo.10282

activity [16,17]. However, some studies have demonstrated non–skeletal-related antitumor activity of N-BPs [18–21], suggesting that bisphosphonates can act directly on tumor cells *in vivo*, probably through inhibition of the prenylation of small GTPases in tumor cells [8].

We have previously suggested that the high affinity of bisphosphonates for bone mineral limits their direct antitumor potential *in vivo* [22]. This assumption is sustained by the observation that the treatment of animals bearing bone metastases with a phosphonocarboxylate analog of the N-BP risedronate, NE-10790, which has a low bone mineral affinity, substantially reduces skeletal tumor growth at a dosage that does not inhibit osteolysis [22]. In this previous study [22], we reasoned that a bisphosphonate possessing weak bone mineral affinity could be released in higher concentration near the bone mineral surface and might act directly on tumor cells that reside in the bone marrow. To further address this question, we propose here to use the opposite strategy and treat animals bearing bone metastases with a bisphosphonate that binds to bone but does not inhibit osteoclast-mediated bone resorption.

We used here risedronate and its structural analog, NE-58051, a bisphosphonate in which the nitrogen-containing side chain is increased by one methylene group inducing a more than 3000-fold decrease of its antiresorptive potency while maintaining a high affinity for the bone mineral [23]. At the molecular level, contrary to risedronate, NE-58051 is a poor inhibitor of FPPS [24]. Here, we compared the effects of risedronate and NE-58051 on cancer cell proliferation *in vitro* and on osteolysis and skeletal tumor growth *in vivo*, using a mouse model of human breast cancer bone metastasis. The effects of a therapy with risedronate or NE-58051 were also compared in animal models of breast cancer tumorigenesis and melanoma lung metastasis.

Materials and Methods

Reagents

Risedronate [2-(3-pyridinyl)1-hydroxyethylidene-bisphosphonic acid] and the analog NE-58051 [3-(3-pyridil)-1-hydroxypropylidene-bisphosphonic acid] were kindly provided by Procter & Gamble Pharmaceuticals (Cincinnati, OH). Stock solutions of bisphosphonates were prepared in phosphate-buffered saline (PBS; pH 7.4; Invitrogen, Paisley, UK), stored at 4°C, and filter-sterilized before use. Farnesol (FOH) and geranylgeraniol (GGOH) were purchased from Sigma (St Louis, MO).

Cells

Breast cancer and melanoma cell lines (MDA-MB-231, ZR-75-1, Hs578T, MCF-7, 4T1, MDA-MB-435s, and B16-F10) were purchased from the American Type Culture Collection (Rockville, MD). The B02-GFP/βGal cell line, a subpopulation of the human MDA-MB-231 breast cancer cell line stably transfected to express luciferase and green fluorescent protein (GFP), which possesses a high propensity to induce osteolytic lesions in nude mice after intravenous tumor inoculation, has been described elsewhere [25,26]. Cells were cultured under standard conditions and maintained in a humidified incubator in an atmosphere of 5% CO_2 at 37°C.

Cell Proliferation Assays

Cell proliferation was determined by 3-(4,5-dimethylthiazol-2-yl)-2,5-diphenyltetrazolium bromide (MTT) assay as previously described [9]. Briefly, cells (500 cells/well) were seeded in 96-well plates and left to adhere for 24 hours. Growing cells were then washed and incubated for 6 days in the absence or in the presence of increasing concentrations (0.001-10 mM) of risedronate or NE-58051. After treatment, cell viability was assessed by the MTT incorporation method. MTT (0.5 mg/ml) is transformed by mitochondrial dehydrogenases in living cells to a blue formazan product spectrophotometrically measurable at 570 nm. Optical density was measured using a 96-well plate reader (MR7000; Dynatech, Chantilly, VA). Half-maximal inhibitory concentration (IC_{50}) of each drug was calculated by logarithmic regression from the dose-response curves. All of the experiments were run in sextuplicate. Results are expressed as mean values ± SD of three independent experiments.

To analyze the effects of the mevalonate pathway intermediates FOH and GGOH on the antiproliferative activity of bisphosphonates, B02-GFP/βGal cells were exposed to risedronate or NE-58051, using their IC_{50} concentrations, in the presence or in the absence of FOH (10 μM) and GGOH (10 μM), respectively. After 6 days of treatment, growth inhibition was analyzed by using a MTT assay, as described above. Data are presented as percentage of control.

Animal Models and Drug Treatments

Four-week-old female BALB/c athymic (*nu/nu*) and C57BL/6 mice were purchased from Charles River (St Germain sur l'Arbresle, France). All procedures involving mice including their housing and care, the method by which they were killed, and experimental protocols were conducted in accordance with a code of practice established by the local ethical committee (Comité Régional d'Ethique pour l'Expérimentation Animale). These studies were routinely inspected by the attending veterinarian to ensure continued compliance with the proposed protocols.

Animal model of bone metastasis. The bone metastasis experiments in mice were conducted as previously described [22,25,26]. Briefly, mice (athymic BALB/c) were randomly assigned to treatment groups, and B02-GFP/βGal cells (5×10^5 cells in 100 μl of PBS) were injected into the tail vein of anesthetized mice on day 0 of the protocol. Risedronate or NE-58051 was given at a daily dose of 150 μg/kg body weight to animals beginning on day 0 and continued until the end of the protocol (day 35). Drugs were administered by subcutaneous injection in 100 μl of PBS (vehicle). Control mice received a daily treatment with vehicle only. On day 35 after tumor cell inoculation, radiographs of anesthetized mice were taken with the use of MIN-R2000 film (Kodak, Rochester, NY) in an MX-20 cabinet x-ray system (Faxitron X-ray Corp, Wheeling, IL), and osteolytic lesions were identified on radiographs as demarcated radiolucent lesions in the bone. The area of osteolytic lesions on the skeleton of each animal was measured using a Visiolab 2000 computerized image analysis system (Explora Nova, La Rochelle, France), and the extent of bone destruction per animal was expressed in square millimeters, as described previously [22,25,26]. Anesthetized mice were killed by cervical dislocation after radiography on day 35, and hind limbs of animals were collected for further histologic analysis.

Animal model of tumorigenesis. B02-GFP/βGal cells (5×10^6 cells in 100 μl of PBS) were inoculated subcutaneously into the right flank of anesthetized BALB/c mice. On day 35 of the protocol, at the time tumor xenografts became palpable, animals were treated subcutaneously with a daily dose of 150 μg/kg risedronate or NE-58051

until the end of the protocol (day 60). Control animals were treated with the vehicle only. Tumor size was measured periodically, and anesthetized mice were killed by cervical dislocation on day 60.

Animal model of lung metastasis. B16-F10 melanoma cells (10^6 cells in 100 μl of PBS) were injected intravenously to anesthetized C57BL/6 mice. NE-58051 (at a dosage of 350 μg/kg per day) was administered to animals by subcutaneous injection beginning on the day of tumor cell inoculation (day 0) and continued until the end of the protocol (day 14). Control animals were treated with the vehicle only. Anesthetized mice were killed by cervical dislocation on day 14, and lungs of animals were collected for further histologic analysis.

In Vivo *Noninvasive Imaging and Image Analysis*

In vivo optical imaging of mice engrafted with B02-GFP/βGal cells was performed as described previously [26]. Briefly, animals bearing B02-GFP/βGal metastases were examined at day 35 after cell inoculation by noninvasive, whole-body fluorescence imaging using a fluorescence scanning system (FluorImager; Amersham Biosciences, Sunnyvale, CA). Scanned images were then analyzed using the computerized image analysis system ImageQuant (Amersham Biosciences).

Microcomputed Tomography Imaging

Hind limbs from animals bearing radiographically confirmed tumors were dissected and fixed in 80% (vol./vol.) alcohol. The bone mineral density of tibiae with radiographic evidence of osteolytic lesions was analyzed by peripheral quantitative computed tomography (CT) with the use of an XCT Research SA+ scanner (Stratec Medizintechnik, Pforzheim, Germany) fitted with a 0.5-mm collimator, as previously described [27].

Bone Histology and Histomorphometry

Bone histologic diagnosis and histomorphometric analysis of bone tissue sections were performed as previously described [25,26]. Briefly, hind limbs from animals fixed in 80% (vol./vol.) alcohol were dehydrated and embedded in methylmethacrylate. A microtome (Polycut E; Reichert-Jung, Heidelberg, Germany) was used to cut 7-μm-thick sections of undecalcified long bones, and the sections were stained with Goldner trichrome [25,26].

Histologic and histomorphometric analyses were performed on Goldner trichrome–stained longitudinal medial sections of tibial metaphysis with the use of a computerized image analysis system (Visiolab 2000), as previously described [25,26]. Histomorphometric measurements (i.e., bone volume–to–tissue volume [BV/TV] and tumor burden–to–soft tissue volume [TB/STV] ratios) were performed in a standard zone of the tibial metaphysis, including cortical and trabecular bones. The BV/TV ratio represents the percentage of bone tissue out of total tissue. The TB/STV ratio represents the percentage of tumor tissue out of total soft tissue.

Measurement of a Biochemical Marker of Bone Turnover

Serum C-terminal cross-linked telopeptide of type I collagen (s-CTX-I), a biochemical marker of collagen degradation, was measured in the bone marrow from mice treated with a bisphosphonate (risedronate or NE-58051) or the vehicle only. Bone marrow from metastatic and nonmetastatic legs was flushed with PBS (100 μl), and CTX-I levels were measured by a competitive ELISA using an antibody raised against an eight–amino acid sequence of type I collagen C-telopeptide (Nordic Bioscience a/s, Herlev, Denmark) according to the manufacturer's protocol.

Statistical Analysis

All data were analyzed with the use of StatView software (version 5.0; SAS Institute, Inc, Cary, NC). Pairwise comparisons were carried out by performing a nonparametric Mann-Whitney *U* test. $P < .05$ were considered statistically significant. All statistical tests were two-sided.

Results

Effects of Risedronate and NE-58051 on Tumor Cell Proliferation

We compared the effects of risedronate and its structural analog NE-58051 (Figure 1*A*), which is 60-fold less potent than risedronate at inhibiting FPPS activity [24], on proliferation of various cancer cell lines. Cells were treated with increasing concentrations of risedronate or NE-58051, and cell viability was measured by MTT assay. Both drugs induced a dose-dependent inhibition of cell growth in all tested cell lines (Figure 1*B*). Irrespective of the cell line used, risedronate was more potent in inhibiting cell proliferation than NE-58051, as demonstrated by their respective IC_{50} (half-maximal inhibitory concentration) values (Table 1). Moreover, cell response to risedronate treatment differed between cell lines, with some cell lines reacting more sensitively to the treatment than others. Conversely, this effect was much less pronounced in NE-58051–treated cells (Table 1 and Figure 1*B*).

We next investigated whether the inhibition of proliferation observed with risedronate and NE-58051 could be reversed by cotreating cells with metabolites of the mevalonate pathway downstream of FPPS: FOH and GGOH. FOH and GGOH are converted to farnesyl diphosphate (FPP) and geranylgeranyl diphosphate (GGPP) in cells; however, unlike FPP and GGPP, the free isoprenols FOH and GGOH are able to enter the cells easily [28] and can thus be used for prenylation of small GTP binding proteins through a salvage pathway. B02-GFP/βGal cells were treated simultaneously with a bisphosphonate at its IC_{50} concentration and 10 μM of FOH or GGOH, respectively. FOH did not reverse the inhibition of proliferation induced by risedronate (Figure 1*C*). However, GGOH partially rescued the proliferation of B02-GFP/βGal cells when added to the culture medium simultaneously with risedronate (58% viability of risedronate/GGOH-treated cells *vs* 28% viability of cells treated with risedronate only; $P < .01$). In contrast, FOH and GGOH had no effect on cell viability of NE-58051–treated cells (Figure 1*C*).

Effects of Risedronate and NE-58051 on the Formation of Breast Cancer Bone Metastases

We used a mouse model of human breast cancer bone metastasis in which animals display radiographic evidence of osteolytic lesions in hind limbs 18 days after tumor cell injection [25,26]. We compared the effects of a daily dosing regimen of risedronate or NE-58051 on the formation of breast cancer bone metastases, using a preventive protocol in which drug administration was initiated on the day of tumor cell inoculation (Figure 2*A*). Radiographic analysis of hind legs at the end of the treatment period (day 35) revealed that mice treated daily with 150 μg of risedronate/kg body weight developed significantly smaller osteolytic lesions compared with mice treated with the same dosing regimen of NE-58051 or with the vehicle (mean area of

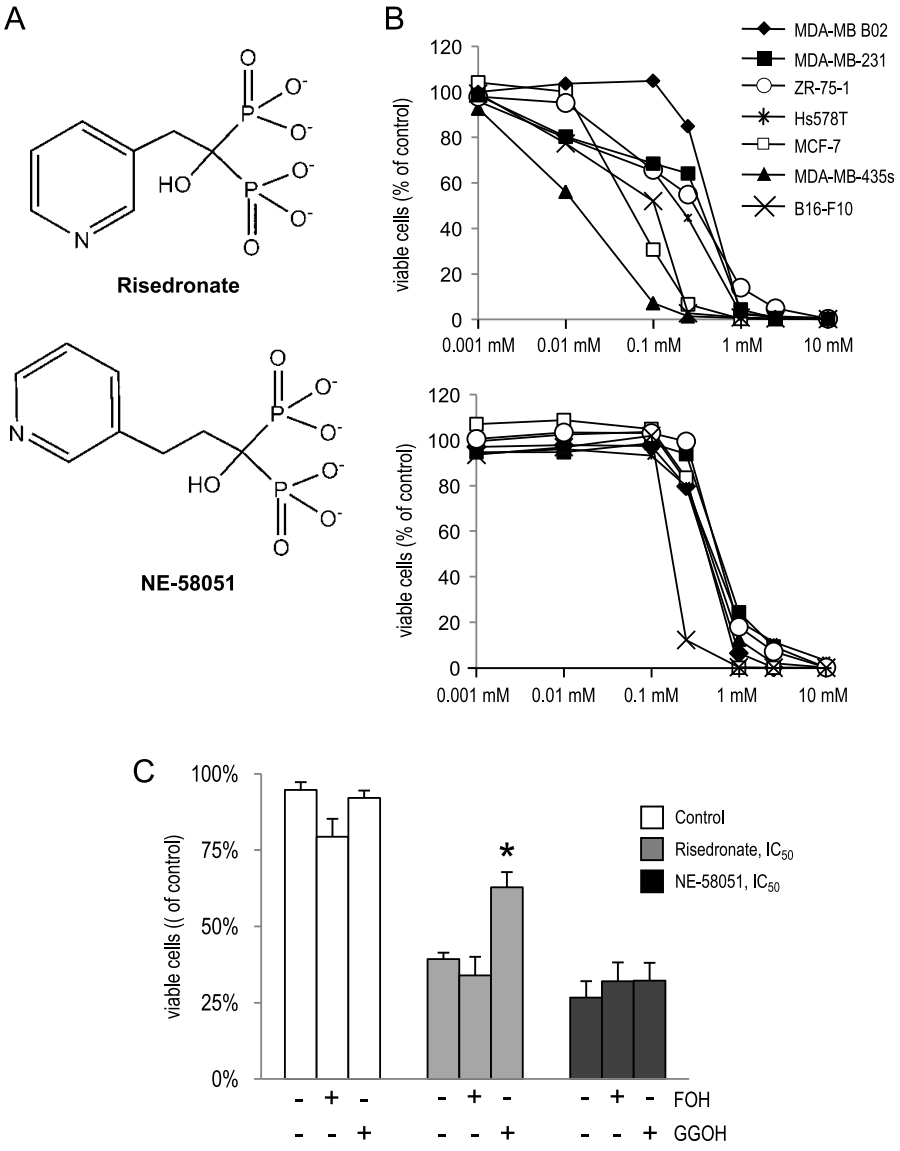

Figure 1. Effects of risedronate and NE-58051 on proliferation of breast and melanoma cells *in vitro*. (A) Chemical structures of risedronate and NE-58051. (B) Dose-dependent inhibition of cancer cell proliferation after a 6-day treatment with 0.001 to 10 mM risedronate or NE-58051, as measured by MTT proliferation assay. Results are the mean of three independent experiments. (C) Effects of the mevalonate pathway intermediates FOH and GGOH on the inhibition of B02-GFP/βGal cell proliferation induced by risedronate or NE-58051. B02-GFP/βGal cells were treated with a bisphosphonate at its IC_{50} concentration with or without adding 10 μM FOH or GGOH, respectively. Results are expressed as the mean OD_{570nm} ± SD of one experiment. *$P < .001$ when compared with the cells treated only with the corresponding drug, using an unpaired Student's *t* test.

osteolytic lesion: risedronate, 0.0 ± 0.0 mm^2; NE-58051, 5.0 ± 0.9 mm^2; vehicle, 4.8 ± 0.6 mm^2; $P < .0005$ for risedronate *vs* vehicle; Table 2 and Figure 2*B*). Reconstruction of hind legs using micro-CT analysis confirmed x-ray results; hind legs from mice treated with risedronate showed a marked increase in bone volume compared with those of mice treated with vehicle or with the daily regimen of NE-58051 (Figure 2*C*). Histomorphometric analysis of metastasis-bearing hind limbs revealed that mice treated with risedronate also had a statistically significantly higher bone volume, as judged by BV/TV ratios, when compared with that observed in mice treated with vehicle (eightfold increase; risedronate, 69.2% ± 3.8% *vs* vehicle, 9.1% ± 1.5%, $P < .005$), whereas mice treated with NE-58051 did not (BV/TV NE-58051,

Table 1. IC_{50} of Risedronate and NE-58051 for Growth Inhibition of Human Breast and Melanoma Cell Lines *In Vitro*.

Cell Line	IC_{50} (mM)*	
	Risedronate [22]	NE-58051
B02-GFP/βGal	0.37 ± 0.04	0.61 ± 0.03
MDA-MB-231	0.24 ± 0.09	0.64 ± 0.04
ZR-75-1	0.25 ± 0.06	0.58 ± 0.13
Hs578T	0.17 ± 0.04	0.49 ± 0.03
MCF-7	0.07 ± 0.01	0.39 ± 0.05
MDA-MB-435s	0.01 ± 0.00	0.46 ± 0.08
B16-F10	0.08 ± 0.02	0.17 ± 0.01

*Results are expressed as the mean ± SD from three independent experiments.

15.0% ± 2.7%; Table 2 and Figure 2*D*). In addition, assessment of bone resorption markers in the bone marrow of mice treated with risedronate showed that a daily treatment with the bisphosphonate significantly reduced CTX-I levels, indicating that risedronate inhibited bone resorption in animals. In contrast, CTX-I levels in NE-58051–treated mice were similar to those of placebo-treated animals (Figure 3).

With regard to skeletal tumor burden, external fluorescence imaging of mice bearing B02 bone metastases revealed that a daily regimen

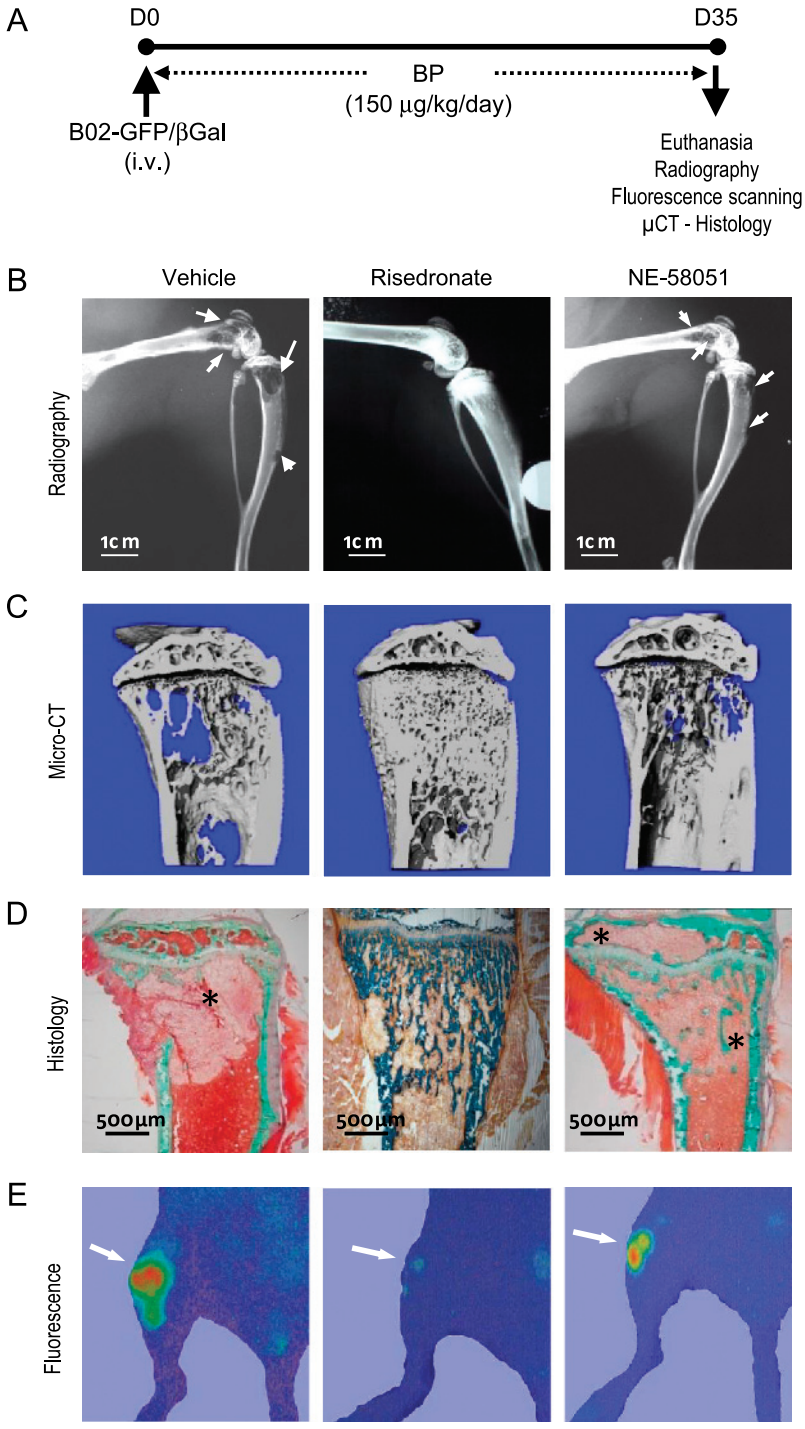

Figure 2. Effects of risedronate and NE-58051 on bone metastasis formation. (A) Treatment protocol for bisphosphonates in a mouse model of human B02 breast cancer cell metastasis to bone. B02-GFP/βGal cells were inoculated intravenously into 4-week-old female BALB/c nude mice on day 0 (D0). Bisphosphonates were administered daily by subcutaneous injection beginning on D0. Mice were killed 35 days after tumor cell inoculation (D35). (B) Representative radiographic images of hind limbs on day 35 after cell inoculation from mice bearing B02-GFP/βGal bone metastases treated with risedronate or NE-58051. Arrows indicate osteolytic lesions. (C) Micro-CT reconstruction of hind limbs obtained from different mice on day 35. Representative images for each group are shown. (D) Micrographs of Goldner trichrome–stained sections of tibial metaphysis. For histologic tissue sections, bone is stained green, whereas bone marrow and tumor cells (asterisk) are stained red. (E) Fluorescence analyses of B02-GFP/βGal tumor cells residing in bone. Arrows indicate fluorescent tumor cells. The images shown are examples that best illustrate the effects of the treatments.

Table 2. Effects of Risedronate and NE-58051 on the Extent of Osteolytic Lesions and Skeletal Tumor Burden in Animals Bearing B02-GFP/βGal Breast Cancer Cells*.

Treatment	Radiography (mm^2/mouse)	Fluorescence (mm^2/mouse)	Histomorphometry	
			BV/TV (%)	TB/STV (%)
Vehicle	4.8 ± 0.6 (n = 11)	20.9 ± 3.0 (n = 11)	9.1 ± 1.5 (n = 9)	20.5 ± 5.6 (n = 9)
Risedronate	0.0 ± 0.0† (n = 7)	6.3 ± 2.4‡ (n = 7)	69.2 ± 3.8† (n = 7)	5.3 ± 3.5† (n = 7)
NE-58051	5.0 ± 0.9 (n = 5)	20.4 ± 3.2 (n = 5)	15.0 ± 2.7 (n = 5)	16.5 ± 9.8 (n = 5)

*Data are expressed as mean values ± SEM from two independent experiments. All measurements were made 35 days after tumor cell injection. *P* values (two-sided) are for pairwise comparisons with vehicle-treated control group using the Mann-Whitney *U* test. *BV/TV* indicates bone volume–to–tissue volume ratio; *TB/STV*, tumor burden (bone metastasis volume)–to–soft tissue volume ratio.
†$P < .0005$, compared with vehicle-treated group.
‡$P < .005$, compared with vehicle-treated group.

of risedronate significantly reduced the number of B02-GFP/βGal cells detected in the hind limbs of animals compared with vehicle-treated mice (area of tumor burden: 6.3 ± 2.4 mm^2 for risedronate *vs* 20.9 ± 3.0 mm^2 for vehicle; Table 2 and Figure 2*E*). In contrast, NE-58051 at the same dosing regimen had no statistically significant inhibitory effect on tumor burden (tumor area, 20.4 ± 3.2 mm^2; Table 2 and Figure 2*E*). Histomorphometric analyses of metastatic hind limbs confirmed fluorescence analyses, showing that a daily regimen of risedronate reduced by 75% the tumor burden, as judged by the measurement of TB/STV ratio, compared with vehicle ($P < .0005$), whereas the TB/STV ratio of mice treated with NE-58051 was similar to that of vehicle-treated animals (Table 2). Furthermore, histologic examination of Goldner trichrome–stained bones from placebo or NE-58051–treated animals showed that an important part of the cancellous bone, as well as some cortical bone in proximal tibiae, was destroyed and replaced by tumor cells that filled the bone marrow cavity (Figure 2*D*). In contrast, cortical bone remained intact and there was a substantial increase in trabecular bone in legs from risedronate-treated animals. In addition, only few small tumor foci were localized in the bone marrow cavity (Figure 2*D*).

Aside from our observation that risedronate decreased skeletal B02-GFP/βGal tumor burden at a dose of 150 μg of risedronate/kg body (Table 2 and Figure 2, *D* and *E*), the effects of a therapy with risedronate or NE-58051 were also compared in animal models of breast cancer tumorigenesis and melanoma lung metastasis. The same total cumulative dose of risedronate or NE-58051 was given to each mouse, regardless of the dosing regimens, which enabled us to directly compare the efficacy of risedronate and NE-58051 among the different animal models of bone and lung metastases, and tumorigenesis. We found that neither risedronate nor NE-58051 was able to inhibit the growth of subcutaneous B02-GFP/βGal tumor xenografts in animals (Figure 4*A*). Moreover, similar to previous results obtained with risedronate [22], NE-58051 given daily at a dose of 350 μg/kg body weight did not inhibit the formation of B16-F10 lung metastases in animals (Figure 4*B*).

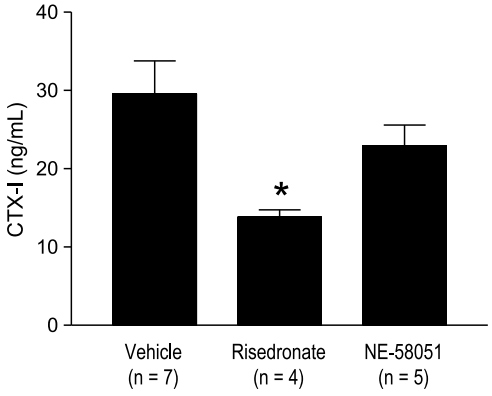

Figure 3. Measurement of CTX-I levels in the bone marrow from mice treated with risedronate, NE-58051, or vehicle only. Bone marrow from metastatic and nonmetastatic legs was flushed, and CTX-I levels were measured by a competitive ELISA using an antibody raised against an eight–amino acid sequence of type I collagen C-telopeptide. Bars indicate the average value. *$P < .05$.

Discussion

N-BPs are highly effective therapeutic agents routinely used for the treatment of bone disorders, particularly tumor-induced bone disease. In addition, N-BPs also have antitumor activity, reducing skeletal tumor burden and inhibiting the formation of bone metastases *in vivo*. However, whether N-BPs achieve this effect by acting directly on tumor cells *in vivo* or indirectly through inhibition of bone resorption remains unclear. Using a phosphonocarboxylate analog of the N-BP risedronate, NE-10790, we have previously shown that a bisphosphonate possessing weak bone mineral affinity is released in higher concentration near the bone mineral surface and acts directly on tumor cells that reside in the bone marrow, reducing skeletal tumor growth at a dosage that does not inhibit osteolysis [22]. In the present study, we used the opposite strategy and compared the antitumor effect of risedronate with that of NE-58051, a structural analog of risedronate with a bone mineral affinity similar to that of risedronate, but having a 3000-fold lower antiresorptive capacity [23,24].

We found that both risedronate and NE-58051 induced a dose-dependent inhibition of cancer cell proliferation *in vitro*. The higher potency of risedronate in inhibiting cancer proliferation, compared with NE-58051, correlated with the higher capacity of this compound to inhibit FPPS activity. These results were in favor of the established view that N-BPs, such as risedronate and zoledronate, act on cancer cells through inhibition of FPPS. NE-58051, however, which lacks the ability to inhibit FPPS, achieved its antiproliferative effect on cancer cell lines through a mechanism independent of the mevalonate pathway. This hypothesis was further supported by our observation that NE-58051–induced growth inhibition of B02-GFP/βGal cells could not be reversed by replenishing cells with metabolites of the mevalonate pathway downstream of FPPS. Conversely, cotreatment with GGOH, which restores geranylgeranylation, partially rescued the inhibition of cell proliferation caused by risedronate. However, if risedronate acted solely through inhibition of FPPS, we would have expected GGOH to have rescued risedronate-treated cancer cells more

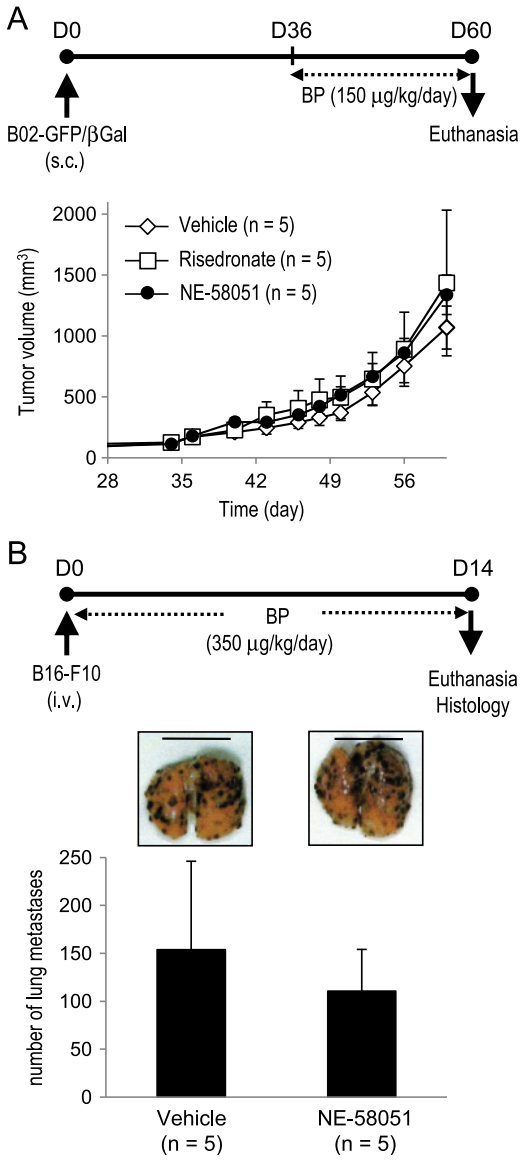

Figure 4. (A) Effect of risedronate and NE-58051 on growth of subcutaneous breast cancer xenografts in nude mice. B02-GFP/βGal cells were inoculated subcutaneously into the right flank of animals. Animals received daily doses of 150 µg/kg risedronate or NE-58051 from day 35, when tumors became palpable, until the end of the protocol (D60). Control animals were treated with the vehicle only. None of the drugs inhibited the growth of B02 breast cancer cells *in vivo*. Results are the mean ± SD of five animals per group. (B) Effect of NE-58051 on lung metastasis formation. B16-F10 melanoma cells were injected intravenously to C57BL/6 mice. NE-58051 (at a dosage of 350 µg/kg per day) was administered to animals by subcutaneous injection beginning on the day of tumor cell inoculation (D0), and continuing until the end of the protocol (D14). Control animals (placebo) were treated with the vehicle only. Visible pigmented melanoma lung metastases were enumerated. Inset: images shown are examples that best illustrate metastatic lungs in each group. NE-58051 did not inhibit B16-F10 lung metastasis. Results are the mean ± SD of five animals per group.

than what we observed. Similar findings have been previously reported with the inhibitory action of the N-BPs pamidronate and olpadronate on osteoclast activity, which are only minimally reversible with GGOH [29]. Altogether, these results ([29] and data presented here) suggest that although bisphosphonates act largely through inhibition of FPPS in cancer cells (and osteoclasts), an additional mechanism independent of the prenylation of small GTPases may occur. This contention is in line with a recent study by Bivi et al. [30] showing that N-BPs (risedronate, alendronate, and ibandronate) target proteins such as tubulin cofactor B and ASK/DBF4 (activator of S-phase kinase). Previous studies have also suggested protein tyrosine phosphatases to be inhibited by alendronate [31,32].

We have previously shown that soluble bisphosphonates are significantly more potent than mineral-bound bisphosphonates at inhibiting tumor cell adhesion to bone *in vitro* [33], and as mentioned before, we also showed that the direct antitumor activity of bisphosphonates is increased *in vivo* by lowering their bone mineral affinity [22]. NE-58051 has a bone mineral affinity similar to that of risedronate [23], and it does not inhibit bone resorption *in vivo* [24]. We showed here that NE-58051 inhibited tumor cell proliferation *in vitro* (Figure 1). However, the treatment of tumor-bearing mice with NE-58051 did not inhibit bone destruction or reduce skeletal tumor burden, as opposed to a bisphosphonate therapy with risedronate. The *in vivo* antitumor activity of risedronate was restricted to bone because it did not inhibit the growth of subcutaneous B02-GFP tumor xenografts (Figure 4*A*) or the formation of B16-F10 melanoma lung metastases [22]. Using CTX as a surrogate marker of bone resorption (Figure 3), risedronate inhibited bone destruction, which subsequently deprived B02 breast cancer cells of bone-derived growth factors required for tumor cell proliferation. Our results are therefore in favor of an indirect antitumor effect of risedronate, once it is bound to bone mineral. However, bisphosphonates do possess antitumor properties [1,8]. For example, zoledronate decreases tumor growth in bone in osteoclast-defective mice [34]. In addition, we have previously shown that bisphosphonate therapy with zoledronate at a high dosage with a long dosing interval reduces osteolysis by inhibiting bone resorption, whereas therapy at a low dosage with a more frequent dosing interval can also directly affect the growth of tumor cells resident in bone [27]. We believe that a frequent low-dose therapy with N-BPs facilitates the prolonged exposure of cancer cells to the drug. Such an assumption is in agreement with the fact that decreasing the bone mineral affinity of bisphosphonates is an effective therapeutic strategy to minimize skeletal tumor growth *in vivo* [22]. Here, given the high daily dose of risedronate administered to animals, we surmise that this N-BP also has the potential to exhibit a direct antitumor effect *in vivo*. However, this direct antitumor effect of risedronate should only occur through inhibition of FPPS activity because NE-58051, under similar experimental conditions, did not exhibit any antitumor activity *in vivo*. The inhibitory mechanisms of N-BPs that are independent of the prenylation of small GTPases therefore seem to play only a minimal role *in vivo*.

In conclusion, our study provides evidence that the antitumor effect of bisphosphonates can be achieved mainly through inhibition of osteoclast-mediated bone resorption. However, once released into the bone marrow cavity, bisphosphonates can also directly target cancer cells through inhibition of the mevalonate pathway. In this regard, the use of compounds with a low bone mineral affinity, which are able to target FPPS, may open new ways to maximize the antitumor activity of bisphosphonates in cancer therapy.

References

[1] Clezardin P, Ebetino FH, and Fournier PGJ (2005). Bisphosphonates and cancer-induced bone disease: beyond their antiresorptive activity. *Cancer Res* **65**, 4971–4974.

[2] Lipton A (2008). Emerging role of bisphosphonates in the clinic—antitumor activity and prevention of metastasis to bone. *Cancer Treat Rev* **34**(suppl 1), S25–S30.

[3] Aapro M, Abrahamsson PA, Body JJ, Coleman RE, Colomer R, Costa L, Crinò L, Dirix L, Gnant M, Gralow J, et al. (2008). Guidance on the use of bisphosphonates in solid tumours: recommendations of an international expert panel. *Ann Oncol* **19**, 420–432.

[4] Coxon FP, Thompson K, and Rogers MJ (2006). Recent advances in understanding the mechanism of action of bisphosphonates. *Curr Opin Pharmacol* **6**, 307–312.

[5] Dunford JE, Thompson K, Coxon FP, Luckman SP, Hahn FM, Poulter CD, Ebetino FH, and Rogers MJ (2001). Structure-activity relationships for inhibition of farnesyl diphosphate synthase *in vitro* and inhibition of bone resorption *in vivo* by nitrogen-containing bisphosphonates. *J Pharmacol Exp Ther* **296**, 235–242.

[6] Roelofs AJ, Thompson K, Gordon S, and Rogers MJ (2006). Molecular mechanisms of action of bisphosphonates: current status. *Clin Cancer Res* **12**, 6222s–6230s.

[7] Green JR (2004). Bisphosphonates: preclinical review. *Oncologist* **9**(suppl 4), 3–13.

[8] Stresing V, Daubiné F, Benzaid I, Mönkkönen H, and Clezardin P (2007). Bisphosphonates in cancer therapy. *Cancer Lett* **257**, 16–35.

[9] Fournier P, Boissier S, Filleur S, Guglielmi J, Cabon F, Colombel M, and Clézardin P (2002). Bisphosphonates inhibit angiogenesis *in vitro* and testosterone-stimulated vascular regrowth in the ventral prostate in castrated rats. *Cancer Res* **62**, 6538–6544.

[10] Wood J, Bonjean K, Ruetz S, Bellahcene A, Devy L, Foidart JM, Castronovo V, and Green JR (2002). Novel antiangiogenic effects of the bisphosphonate compound zoledronic acid. *J Pharmacol Exp Ther* **302**, 1055–1061.

[11] Bezzi M, Hasmim M, Bieler G, Dormond O, and Ruegg C (2003). Zoledronate sensitizes endothelial cells to tumor necrosis factor–induced programmed cell death: evidence for the suppression of sustained activation of focal adhesion kinase and protein kinase B/Akt. *J Biol Chem* **278**, 43603–43614.

[12] Kunzmann V, Bauer E, Feurle J, Weißinger F, Tony HP, and Wilhelm M (2000). Stimulation of γδ T cells by aminobisphosphonates and induction of antiplasma cell activity in multiple myeloma. *Blood* **96**, 384–392.

[13] Dieli F, Gebbia N, Poccia F, Caccamo N, Montesano C, Fulfaro F, Arcara C, Valerio MR, Meraviglia S, Di Sano C, et al. (2003). Induction of γδ T-lymphocyte effector functions by bisphosphonate zoledronic acid in cancer patients *in vivo*. *Blood* **102**, 2310–2311.

[14] Käkönen SM and Mundy GR (2003). Mechanisms of osteolytic bone metastases in breast carcinoma. *Cancer* **97**, 834–839.

[15] Fromigue O, Kheddoumi N, and Body JJ (2003). Bisphosphonates antagonize bone growth factors' effects on human breast cancer cells survival. *Br J Cancer* **89**, 178–184.

[16] van der Pluijm G, Que I, Sijmons B, Buijs JT, Lowik CW, Wetterwald A, Thalmann GN, Papapoulos SE, and Cecchini MG (2005). Interference with the microenvironmental support impairs the *de novo* formation of bone metastases *in vivo*. *Cancer Res* **65**, 7682–7690.

[17] Zheng Y, Zhou H, Brennan K, Blair JM, Modzelewski JR, Seibel MJ, and Dunstan CR (2007). Inhibition of bone resorption, rather than direct cytotoxicity, mediates the anti-tumour actions of ibandronate and osteoprotegerin in a murine model of breast cancer bone metastasis. *Bone* **40**, 471–478.

[18] Giraudo E, Inoue M, and Hanahan D (2004). An amino-bisphosphonate targets MMP-9–expressing macrophages and angiogenesis to impair cervical carcinogenesis. *J Clin Invest* **114**, 623–633.

[19] Yamagishi S, Abe R, Inagaki Y, Nakamura K, Sugawara H, Inokuma D, Nakamura H, Shimizu T, Takeuchi M, Yoshimura A, et al. (2004). Minodronate, a newly developed nitrogen-containing bisphosphonate, suppresses melanoma growth and improves survival in nude mice by blocking vascular endothelial growth factor signaling. *Am J Pathol* **165**, 1865–1874.

[20] Ory B, Heymann MF, Kamijo A, Gouin F, Heymann D, and Redini F (2005). Zoledronic acid suppresses lung metastases and prolongs overall survival of osteosarcoma bearing mice. *Cancer* **104**, 2522–2529.

[21] Hiraga T, Williams PJ, Ueda A, Tamura D, and Yoneda T (2004). Zoledronic acid inhibits visceral metastases in the 4T1/luc mouse breast cancer model. *Clin Cancer Res* **10**, 4559–4567.

[22] Fournier PG, Daubiné F, Lundy MW, Rogers MJ, Ebetino FH, and Clézardin P (2008). Lowering bone mineral affinity of bisphosphonates as a therapeutic strategy to optimize skeletal tumor growth inhibition *in vivo*. *Cancer Res* **68**, 8945–8953.

[23] van Beek ER, Löwik CWGM, Ebetino FH, and Papapoulos SE (1998). Binding and antiresorptive properties of heterocycle-containing bisphosphonate analogs: structure-activity relationships. *Bone* **23**, 437–442.

[24] Dunford JE, Kwaasi AA, Rogers MJ, Barnett BL, Ebetino FH, Russell RG, Oppermann U, and Kavanagh KL (2008). Structure-activity relationships among the nitrogen containing bisphosphonates in clinical use and other analogues: time-dependent inhibition of human farnesyl pyrophosphate synthase. *J Med Chem* **51**, 2187–2195.

[25] Pécheur I, Peyruchaud O, Serre CM, Guglielmi J, Voland C, Bourre F, Margue C, Cohen-Solal M, Buffet A, Kiefer N, et al. (2002). Integrin $\alpha_v\beta_3$ expression confers on tumor cells a greater propensity to metastasize to bone. *FASEB J* **16**, 1266–1268.

[26] Peyruchaud O, Serre CM, NicAmhlaoibh R, Fournier P, and Clézardin P (2003). Angiostatin inhibits bone metastasis formation in nude mice through a direct anti-osteoclastic activity. *J Biol Chem* **278**, 45826–45832.

[27] Daubiné F, Le Gall C, Gasser J, Green J, and Clézardin P (2007). Antitumor effects of clinical dosing regimens of bisphosphonates in experimental breast cancer bone metastasis. *J Natl Cancer Inst* **99**, 322–330.

[28] Crick DC, Andres DA, and Waechter CJ (1997). Novel salvage pathway utilizing farnesol and geranylgeraniol for protein isoprenylation. *Biochem Biophys Res Commun* **237**, 483–487.

[29] van Beek ER, Cohen LH, Leroy IM, Ebetino FH, Löwik CWGM, and Papapoulos SE (2003). Differentiating the mechanisms of antiresorptive action of nitrogen containing bisphosphonates. *Bone* **33**, 805–811.

[30] Bivi N, Romanello M, Harrison R, Clarke I, Hoyle DC, Moro L, Ortolani F, Bonetti A, Quadrifoglio F, Tell G, et al. (2009). Identification of secondary targets of N-containing bisphosphonates in mammalian cells via parallel competition analysis of the barcoded yeast deletion collection. *Genome Biol* **10**, R93.

[31] Schmidt A, Rutledge SJ, Endo N, Opas EE, Tanaka H, Wesolowski G, Leu CT, Huang Z, Ramachandaran C, Rodan SB, et al. (1996). Protein-tyrosine phosphatase activity regulates osteoclast formation and function: inhibition by alendronate. *Proc Natl Acad Sci USA* **93**, 3068–3073.

[32] Skorey K, Ly HD, Kelly J, Hammond M, Ramachandran C, Huang Z, Gresser MJ, and Wang Q (1997). How does alendronate inhibit protein-tyrosine phosphatases? *J Biol Chem* **272**, 22472–22480.

[33] Boissier S, Ferreras M, Peyruchaud O, Magnetto O, Ebetino FH, Colombel M, Delmas P, Delaissé JM, and Clézardin P (2000). Bisphosphonates inhibit breast and prostate carcinoma cell invasion, an early event in the formation of bone metastases. *Cancer Res* **60**, 2949–2954.

[34] Hirbe AC, Roelofs AJ, Floyd DH, Deng H, Becker SN, Lanigan LG, Apicelli AJ, Xu Z, Prior JL, Eagleton MC, et al. (2009). The bisphosphonate zoledronic acid decreases tumor growth in bone in mice with defective osteoclasts. *Bone* **44**, 908–916.